JOURNAL OF CATALYSIS 134, 702–712 (1992)

Incorporation of La^{3+} into a $Rh/\gamma\text{-}Al_2O_3$ Catalyst

R. K. USMEN, R. W. MCCABE, L. P. HAACK, G. W. GRAHAM, J. HEPBURN, AND W. L. H. WATKINS

Ford Motor Company, P.O. Box 2053, Dearborn, Michigan 48121

Received June 7, 1991; revised October 2, 1991

The effects of La^{3+} incorporation into $Rh/\gamma\text{-}Al_2O_3$ were investigated by a combination of temperature-programmed reduction, X-ray photoelectron spectroscopy, CO chemisorption, and reactivity measurements. The reduction of Rh^{3+} following high-temperature (>600°C) oxidation was more facile and the dispersion of Rh was higher with La^{3+} present. Notwithstanding, the catalytic activity, as manifested by the HC, CO, and NO_x conversion efficiencies, was lower in the presence of La^{3+}. This is attributed to a combination of Rh particle-size effects and possible La–Rh compound formation under oxidizing conditions. Changes brought about by high-temperature oxidation in catalysts both with and without La^{3+} were completely reversed by high-temperature reduction.

INTRODUCTION

The current catalysts used for the control of automotive emissions contain Rh, primarily to promote the reduction of NO_x (*1*). The high cost and the limited availability of Rh provide a strong incentive to develop methods for its more effective utilization. It has been found that Rh, dispersed on a $\gamma\text{-}Al_2O_3$ support, interacts with the support when exposed to high temperatures resulting in a loss of activity (*2*). The most pronounced deactivation of Rh-containing catalysts occurs at temperatures >600°C, particularly in oxidizing environments (*2, 3*). Recent studies using infrared spectroscopy, temperature-programmed reduction, *in situ* transmission electron microscopy, and *in situ* dispersion and reactivity measurements confirm that in oxidizing environments at high temperature, rhodium (or rhodium oxide) diffuses into $\gamma\text{-}Al_2O_3$ or changes to some form that is very difficult to reduce (*4–6*). Other supports, such as $\alpha\text{-}Al_2O_3$ or ZrO_2, are known to be more resistant to this form of deactivation, however (*7*).

Several recent studies suggest that alternative support compositions might also be used to promote Rh activity (*1, 8–11*). It has been shown that Rh/TiO_2 is more active than Rh/SiO_2 for NO reduction by CO (*1, 8, 9*) and Rh, Pt, and Pd supported on TiO_2 are more active for NO reduction by CO than catalysts prepared on supports like SiO_2 or Al_2O_3 (*10*). Enhanced catalytic activities and promoter effects have been reported by combining noble metals (Pd, Pt, Rh) with rare earth oxides (La_2O_3, Nd_2O_3, CeO_2) (*10, 11*).

The present investigation was undertaken to examine the influence of La^{3+} ions on the rhodium-support interaction. To this extent, lanthana was employed strictly as a surface modifier and not as a bulk stabilizer of the alumina surface area, as conventionally employed (*12*). Specifically, the experiments were designed to test a simple hypothesis. If the interaction of Rh with $\gamma\text{-}Al_2O_3$ involves dissolution of Rh^{3+} ions into the $\gamma\text{-}Al_2O_3$, is it possible to block this dissolution? In other words, might La^{3+} ions preferentially interact with the $\gamma\text{-}Al_2O_3$, thus preventing the dissolution of Rh^{3+} ions under high-temperature oxidizing conditions? A strong interaction of La^{3+} with the $\gamma\text{-}Al_2O_3$ surface is

0021-9517/92 $3.00

known to exist (*13*). A second goal was to examine the possible promoting effect of La^{3+} on the activity of $Rh/\gamma\text{-}Al_2O_3$. The catalytic activities of samples both with and without La^{+3} and with and without exposure to high-temperature oxidizing and reducing environments were thus determined. The activities were correlated with results from temperature-programmed reduction (TPR), X-ray photoelectron spectroscopy (XPS), and CO chemisorption measurements.

EXPERIMENTAL DETAILS

Catalyst Preparation

A 10 wt% $La_2O_3/\gamma\text{-}Al_2O_3$ sample was prepared by impregnating $\gamma\text{-}Al_2O_3$ powder (Aesar, Johnson Matthey, Inc.) with $La(NO_3)_3 \cdot 6H_2O$ solution of appropriate concentration by the incipient wetness method. The sample was dried at 100°C and calcined at 550°C for 4 h. The 0.6 wt% Rh catalysts were prepared by impregnating $\gamma\text{-}Al_2O_3$ powder and the 10 wt% $La_2O_3/\gamma\text{-}Al_2O_3$ sample with $Rh(NO_3)_3 \cdot 2H_2O$ solution of the appropriate concentration by the incipient wetness method. The catalysts were dried at 100°C and calcined at 550°C for 4 h.

Catalyst Pretreatment

The catalysts prepared by the methods outlined above are referred to as "fresh" catalysts in this report. The samples of the fresh catalysts were subjected to additional pretreatment prior to use. The nomenclature and the pretreatment conditions for 0.6 wt% $Rh/\gamma\text{-}Al_2O_3$ and 0.6 wt% Rh/10 wt% $La_2O_3/\gamma\text{-}Al_2O_3$ catalysts are summarized in Fig. 1. The sample pretreatment for TPR, XPS, and reactivity measurements consisted of heating the fresh sample in flowing hydrogen up to 800°C at 15°C/min, cooling to 500°C, and soaking in hydrogen at 500°C for 1 h, followed by oxidation at 500°C in flowing oxygen for 1 h. The sample was cooled in helium and was designated as 500°C, O_2 sample. Portions of the 500°C, O_2 sample were subsequently reduced and oxidized at 800 and 900°C, respectively, and

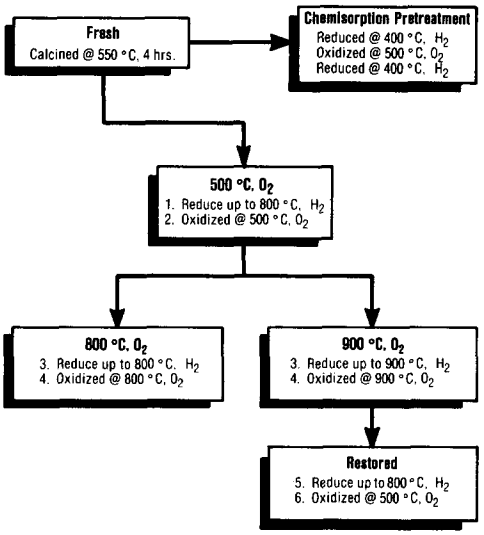

FIG. 1. Summary of sample pretreatment.

are labeled 800°C, O_2 and 900°C, O_2 samples as shown in Fig. 1. Aging was limited to 900°C at most since the transitional alumina, which we use as support material, is stabilized at a BET surface area of ~100 m^2/g by calcining at 900°C or higher.

The sample pretreatment for CO chemisorption measurements consisted of reduction of the fresh catalyst in hydrogen at 400°C for 2 h, followed by exposure to oxygen at 500°C for 2 h and a second reduction in hydrogen at 400°C, followed by evacuation.

Temperature-Programmed Reduction

TPR experiments were carried out on an Altamira temperature-programmed system. The TPR apparatus has been described in detail previously (*14*). Oxidizing pretreatments were carried out in the TPR cell in a 40 cc/min flow of 10% O_2 in He at each specified pretreatment temperature (Fig. 1) for 1 h. The samples were then cooled in flowing He to room temperature before the temperature-programmed reduction was started. The TPR profiles were obtained by ramping the temperature at 15°C/min and measuring the H_2 uptake with a thermal con-

ductivity detector. The overall H_2 uptakes were obtained by integrating the TPR profiles.

X-Ray Photoelectron Spectroscopy

XPS was performed using an M-Probe spectrometer manufactured by Surface Science Instruments (Mountain View, CA). Spectra were acquired using monochromatic Al$K\alpha$ (1486.6 eV) radiation with the analyzer operated at a 150-eV pass energy. A low-energy (1–3 eV) electron flood gun in combination with a Ni charge neutralization screen were employed to minimize surface charging. The base pressure of the spectrometer was 2×10^{-9} Torr. Core level binding energies were referenced to the support Al 2p line at 74.2 eV. Analyses were performed on samples of the pretreated catalysts that had been pressed into pellets (6 mm diameter, ~1 mm thick).

The data system used was also supplied by Surface Science Instruments. Quantification of survey data was accomplished by means of routines based on Scofield photoionization cross-section values. High-resolution spectra were fitted using a least-squares fitting routine to accurately determine core level binding energy positions. The binding energies were measured with an accuracy of ±0.2 eV.

The samples, as prepared in Fig. 1, were loaded into a PHI Model 04-800 catalytic reactor system mounted directly onto the sample preparation chamber of the M-Probe spectrometer. The base pressures of the preparation chamber and reactor were 1×10^{-9} Torr and 5×10^{-8} Torr, respectively. The reactor gases used were O_2 (99.98%) and H_2 (99.9995%), purchased from Matheson (Chicago, IL). Reactions were carried out in 1 atm of gas using a flow rate of ~50 cm^3/min. Samples were transferred directly from the reactor to the analyzer *in vacuo* to eliminate contamination due to air exposure.

Samples initially were reoxidized *in situ* at 500°C for 90 min before analysis by XPS in order to outgas them and also remove carbon contamination. Stepwise reductions were then carried out to parallel the TPR experiments. The first reduction step was achieved by heating from room temperature (~20°C) to 200°C at a temperature increase of 15°C/min. When 200°C was achieved, the reactor was purged immediately with Ar gas, cooled to room temperature, and then opened to vacuum for XPS analysis. A second reduction step to a final temperature of 400°C was carried out similarly. The choice of these reduction temperatures was based on the position of peaks in the TPR results, as indicated below. Finally, a prolonged reduction step was performed by holding the reactor temperature at 600°C for 60 min, and then proceeding as before.

Chemisorption

A conventional vacuum apparatus consisting of calibrated glass bulbs and a quartz-spiral manometer (Heise Instruments) was used for chemisorption measurements. The chemisorption apparatus has been described in detail previously (*15*). The apparent volume of the adsorption vessel was obtained from the pressure change of helium expanding from a standard volume. CO was used as adsorbate for the chemisorption measurements, performed at room temperature.

Surface areas of the fresh catalysts were determined by the BET technique with a Quantachrome instrument. The BET surface areas, measured by N_2 adsorption, are summarized in Table 1.

Flow Reactor

A laboratory flow reactor was used to evaluate the activity of the samples. The activities were measured at 550°C at a space velocity of 60,000 h^{-1}. The feed gas composition, simulating an engine exhaust gas near stoichiometry, was 1.5 vol% CO, 0.5 vol% H_2, 1500 vol. ppm HC (consisting of 1000 vol. ppm C_3H_6 and 500 vol. ppm C_3H_8), 1000 vol. ppm NO, 0.6 vol% to 1.4 vol% O_2, 20 vol. ppm SO_2, and balance N_2. R, the molar ratio of reducing species to oxidizing species

TABLE 1

BET and Chemisorption Analysis of 500°C, O_2 Samples

Sample	BET (m^2/g)	CO uptake $\mu mol/m^2$ BET	% Rh exposed
$Rh/\gamma\text{-}Al_2O_3$	74	.236	18
$Rh/La_2O_3/\gamma\text{-}Al_2O_3$	82	.417	36

in the feed ($R < 1$ = lean; $R = 1$ = stoichiometric; $R > 1$ = rich), was varied by changing the amount of O_2 in the feed. The analytical section of the reactor system consisted of detectors for NO (Beckman Model 951A), CO (Beckman Model 864), O_2 (SensorMedics OM-11 EA), and HC (Beckman Model 400A).

RESULTS

Temperature-Programmed Reduction

The reduction profiles for the 0.6 wt% $Rh/\gamma\text{-}Al_2O_3$ catalyst following the various oxidation pretreatments are presented in Fig. 2. The reduction profile for the 500°C, O_2 sample consisted of two main peaks centered around 87 and 624°C. The integrated area of the low-temperature peak, associated with reduction of accessible Rh_2O_3, accounted for essentially all Rh^{3+} in the sample, as shown in Table 2. The low-temperature peak area decreased sharply with increased oxidation temperature. During TPR of the 900°C, O_2 sample, for example, this peak represented only 8.7% of the total Rh^{3+} present in the sample. The origin of the high-temperature peak in the profile from the 500°C, O_2 sample is unknown; however, it was not observed in TPR experiments carried out on blank alumina, which showed no significant TPR features up to 800°C.

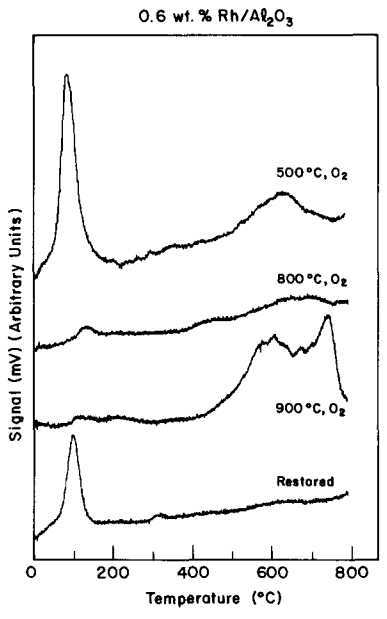

FIG. 2. TPR spectra of 0.6 wt $Rh/\gamma\text{-}Al_2O_3$ samples after various oxidation pretreatments.

The amount of accessible Rh_2O_3 in the 900°C, O_2 sample could be increased by subsequently reducing the sample at 800°C followed by reoxidation at 500°C (Fig. 2). The reduction profile for the restored sample is nearly identical to that of the 500°C, O_2 sample. (The peak areas do not look equivalent because of different sample sizes.) Furthermore, Table 2 shows that nearly identical quantities of H_2 were consumed during the reduction of the 500°C, O_2 (low-temperature oxidized) and restored (after high-temperature reduction) samples. The small difference between these values is within the uncertainty associated with the baseline and slope corrections of the TPR spectra.

Figure 3 shows the TPR profiles for the 0.6 wt% Rh/10 wt% $La_2O_3/\gamma\text{-}Al_2O_3$ catalysts following various oxidation pretreatments. Consistent with the $Rh/\gamma\text{-}Al_2O_3$ catalysts, the reduction profile for the 500°C, O_2 sample contained two peaks centered around

TABLE 2

Analysis of Low-Temperature TPR Peak

Sample	H_2 consumption (μmol/g catalyst)	T(°C)	% Rh reduced[a]
0.6 wt% Rh/γ-Al_2O_3			
500°C, O_2	94.8	87	93.4
800°C, O_2	21.6	127	22.8
900°C, O_2	8.2	130	8.7
Restored	92.4	95	97.5
0.6 wt% Rh/10 wt% La_2O_3/γ-Al_2O_3			
500°C, O_2	110.8	117	78.7
800°C, O_2	57.5	183, 294	51.9
900°C, O_2	43.9	287	39.6
Restored	89.1	103	80.4

[a] Assuming uptake entirely due to $Rh^{3+} \rightarrow Rh^0$.

117 and 638°C. The low-temperature peak vanished and new broad peaks appeared at higher temperatures (183 and 287°C) as the oxidation temperature increased. The new features that are seen in the TPR spectra of these high-temperature oxidized samples could indicate the formation of new species (possibly a Rh–La compound) at higher oxidation temperatures. This TPR result is consistent with a recent study (*9*) of bulk mixed oxides of Rh^{3+} and other cations, where it has been shown that Rh^{3+} strongly interacts with La and Ce cations, becoming more difficult to reduce than Rh_2O_3. Furthermore, Table 2 suggests that the $Rh/La_2O_3/\gamma$-Al_2O_3 catalyst may retain more Rh^{3+} in a form that is reducible at temperatures below 350°C than the corresponding Rh/γ-Al_2O_3 catalyst (for example, 39.6% of the total oxidized Rh in the 900°C, O_2 $Rh/La_2O_3/\gamma$-Al_2O_3 sample as compared to only 8.7% in the 900°C, O_2 Rh/γ-Al_2O_3 sample). Evidently, the addition of La^{3+} blocks, to some extent, interaction of the Rh with the γ-Al_2O_3 support and results in the retention of a greater amount of reducible Rh^{3+} on the surface following high-temperature oxidation.

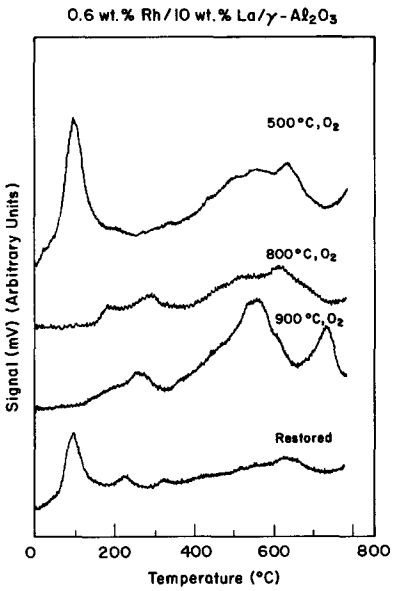

FIG. 3. TPR spectra of 0.6 wt% Rh/10 wt% La_2O_3/γ-Al_2O_3 samples after various oxidation pretreatments.

As with the Rh/γ-Al_2O_3 catalyst, some additional TPR features of unknown origin were observed for the $Rh/La_2O_3/\gamma$-Al_2O_3 catalyst at temperatures above 500°C. Some of these may be associated with the modified support itself, as TPR experiments with the blank La_2O_3/γ-Al_2O_3 yielded peaks near 580 and 710°C.

XPS

The XPS results from the 0.6 wt% Rh/γ-Al_2O_3 samples are shown in Fig. 4. In each

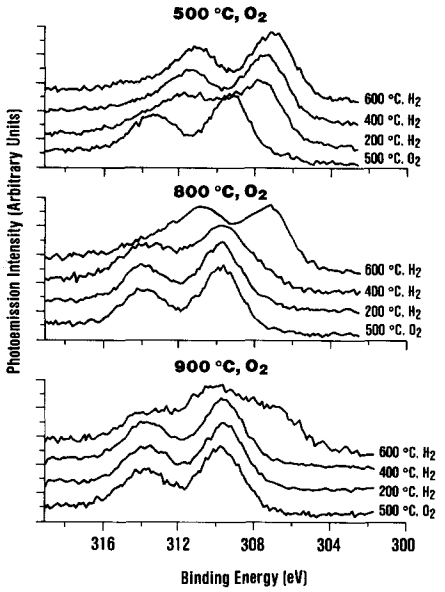

FIG. 4. Rh(3*d*) core level spectra of 0.6% $Rh/\gamma\text{-}Al_2O_3$.

of the three sets of Rh 3*d* spectra, corresponding to a sample with a given pretreatment and then subjected to stepwise reduction at progressively higher temperatures, it is apparent that the Rh, oxidized at first, tends toward the metallic state. The binding energy shift between metal and oxide is much larger than expected for Rh_2O_3, however, as further discussed below. In the case of the 500°C, O_2 sample, the reduction is almost complete after a 200°C reduction, while for the 900°C, O_2 sample, only about half of the Rh^{3+} has been reduced after a (prolonged) 600°C reduction. The case of the 800°C, O_2 sample, is intermediate. In addition, the total integrated intensity of the Rh 3*d* core levels, normalized to the Al 2*p* core-level intensity, is roughly constant for all three samples, independent of treatment, as shown in Fig. 5. This implies relatively little redistribution of Rh^{3+}, either upon reduction or oxidation at high temperature. The latter observation supports the view that any penetration of Rh^{3+} into the alumina does not extend to a depth of more than a few atomic layers, since otherwise it would contribute little to the XPS signal.

The XPS results from the 0.6 wt% Rh/10 wt% $La_2O_3/\gamma\text{-}Al_2O_3$ samples, shown in Fig. 6, are similar to those of Fig. 4. One difference, however, concerns the degree to which the initial oxide tends to be reduced. In the case of the 900°C, O_2 sample, there has been somewhat more oxide reduced by 400°C and much more by 600°C than in the corresponding situations for the sample without La^{3+}. In addition, while the total integrated intensity of the Rh 3*d* core levels, normalized to the Al 2*p* core-level intensity, is again roughly constant for all three samples, independent of treatment, it is about 50% larger than that of the samples without La^{3+} (Fig. 5). (Inclusion of La in the normalization has almost no effect since the measured La/Al atomic ratio was only 0.06.) This is consistent with a higher Rh dispersion, demonstrated by the CO chemisorption results presented below.

Concerning the magnitude of the Rh 3*d*

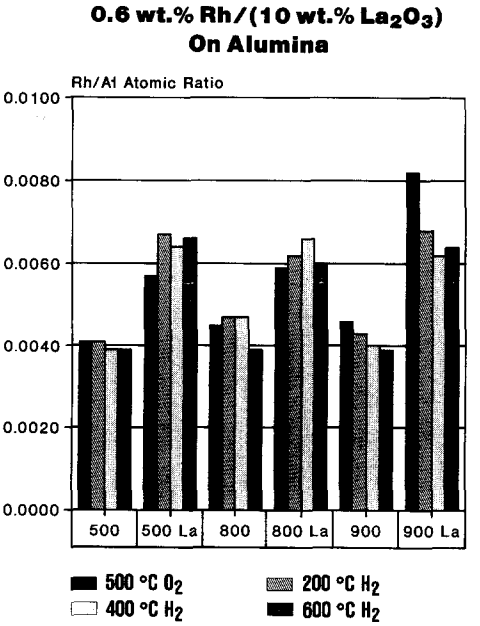

FIG. 5. Quantification of Rh concentration obtained from XPS measurements of Rh(3*d*) core level intensity (normalized by aluminum 2*p* core level intensity). The Rh/Al atomic ratio based on the bulk concentrations is 0.003.

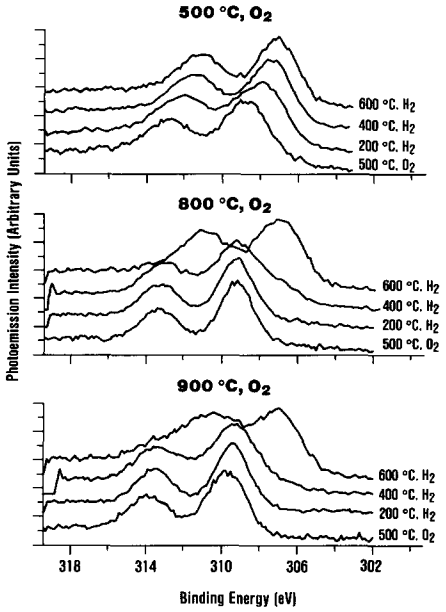

FIG. 6. Rh(3*d*) core level spectra of 0.6 wt% Rh/10 wt% La_2O_3/γ-Al_2O_3.

core-level shift between metal and oxide, we note that the value generally observed here, 2.7 eV, is more than 1 eV larger than the shift measured for bulk Rh_2O_3, 1.6 eV (*9*). A similar result has also been reported by Beck and Carr (*16*). We have no good explanation for this but attribute it (as well as the anomalously large peak widths) to an effect of high dispersion. Differences in the Rh 3*d* core-level shift for Rh_2O_3 and $LaRhO_3$, known to be only about 0.2 eV in the bulk, would not be apparent here.

Chemisorption

CO chemisorption results are presented in Fig. 7. The chemisorption measurements were carried out after the pretreatment described in the experimental section and the data were analyzed to yield the dispersion results shown in Table 1, using the measured BET surface areas, also shown in Table 1. These results are based on the ratio $CO_{\text{chemisorbed}} : Rh_{\text{subsurface atoms}} = 1.65$ measured by Yao *et al.* (*3*) and Oh (*17*) for similar loadings of Rh. The apparent percentage

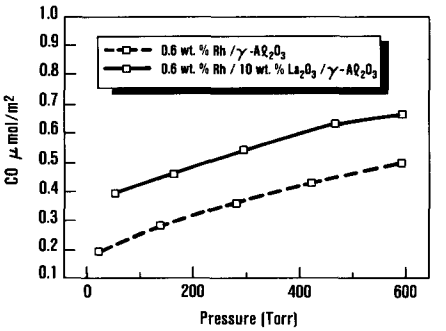

FIG. 7. CO chemisorption on 0.6 wt% Rh/γ-Al_2O_3 and 0.6 wt% Rh/10 wt% La_2O_3/γ-Al_2O_3.

dispersion was twice as high for the 0.6 wt% Rh/10 wt% La_2O_3/γ-Al_2O_3 catalyst as for the 0.6 wt% Rh/γ-Al_2O_3 catalyst (36 and 18, respectively). We caution that the calculated dispersions should perhaps best be viewed as relative measures for the two catalysts owing to uncertainties in the adsorption stoichiometry. Moreover, we cannot rule out the possibility that increased adsorption of CO on the support could be occurring in the case of the lanthana modified catalyst, thereby affecting the apparent dispersion.

Catalytic Activities

The catalytic activities of Rh/γ-Al_2O_3 and $Rh/La_2O_3/\gamma$-Al_2O_3 samples oxidized at vari-

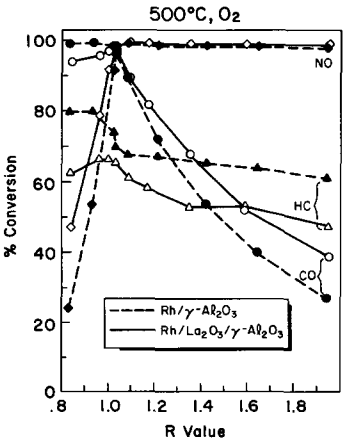

FIG. 8. Catalytic activities of Rh/γ-Al_2O_3 and $Rh/La_2O_3/\gamma$-Al_2O_3 samples oxidized at 500°C.

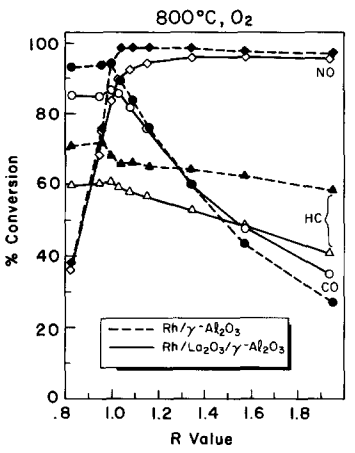

FIG. 9. Catalytic activities of $Rh/\gamma\text{-}Al_2O_3$ and $Rh/La_2O_3/\gamma\text{-}Al_2O_3$ samples oxidized at 800°C.

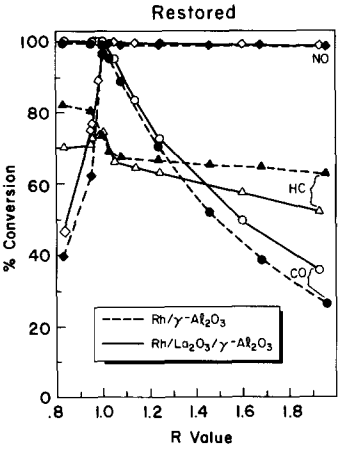

FIG. 11. Catalytic activities of $Rh/\gamma\text{-}Al_2O_3$ and $Rh/La_2O_3/\gamma\text{-}Al_2O_3$ samples after high-temperature reduction followed by 500°C oxidation treatment (restored samples).

ous temperatures are compared in Figs. 8–10. Conversions of HC, CO, and NO are plotted as a function of R. The overall HC conversion of the $Rh/La_2O_3/\gamma\text{-}Al_2O_3$ sample was lower than that of the $Rh/\gamma\text{-}Al_2O_3$ sample both as prepared (Fig. 8) and after preoxidation at 800°C (Fig. 9) and 900°C (Fig. 10). Even after high-temperature reduction–low-temperature oxidation treatment (to restore the amount of reducible Rh), the HC conversion of the $Rh/La_2O_3/\gamma\text{-}Al_2O_3$ sample was less than that of its $Rh/\gamma\text{-}Al_2O_3$ counterpart except near $R = 1$ (Fig. 11).

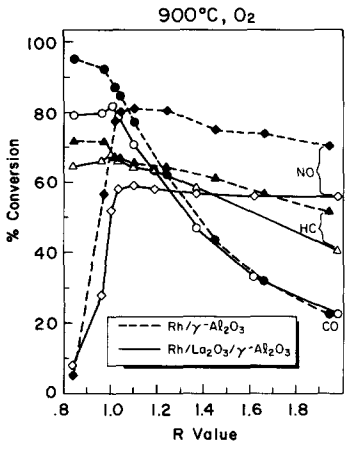

FIG. 10. Catalytic activities of $Rh/\gamma\text{-}Al_2O_3$ and $Rh/La_2O_3/\gamma\text{-}Al_2O_3$ samples oxidized at 900°C.

Note that the HC conversions obtained with the $Rh/\gamma\text{-}Al_2O_3$ catalyst under lean conditions ($R < 1$) were consistently above 70%, indicating essentially complete conversion of propylene and up to 55% conversion of more difficult-to-oxidize propane. In contrast, the total HC conversion of the La^{3+}-containing catalyst never exceeded 70% over the 500, 800, and 900°C oxidized samples, indicating at most about 10% conversion of propane.

In addition to lower HC conversion, the 500°C $Rh/La_2O_3/\gamma\text{-}Al_2O_3$ catalyst (Fig. 8) showed lower lean-side CO conversion, but greater lean-side NO conversion and rich-side CO conversion than its $Rh/\gamma\text{-}Al_2O_3$ counterpart. The higher rich-side CO activity corresponds in magnitude to the additional O_2 available because of the lower rich-side HC conversion of the La-containing catalyst, and thus appears only to be a consequence of the different exhaust composition and not the catalyst itself. With high-temperature oxidation (Figs. 9 and 10), the most dramatic change was a large decrease in NO conversion of the La-containing catalyst compared to the catalyst without La. Lean-side CO conversion was also much lower for the lanthana-

containing catalyst compared to the Rh/γ-Al_2O_3 catalyst.

The catalytic activities for HC, CO, and NO conversions of both samples were restored to equivalent or higher conversions after high-temperature reduction–low-temperature oxidation treatment (compare Figs. 8 and 11).

DISCUSSION

For the 500°C oxidized samples of Rh/γ-Al_2O_3 and Rh/La_2O_3/γ-Al_2O_3, the TPR results indicate that nearly all of the Rh is present at the surface of the alumina in a readily reducible form. The presence of La^{3+} had no affect on the amount of reducible Rh at 500°C. From an activity standpoint, the addition of La^{3+} to the Rh catalyst primarily inhibited HC oxidation, but also affected lean-side NO and CO activity and enhanced rich-side CO oxidation (presumably due to a greater availability of O_2 resulting from the lower HC conversion).

The inhibiting effect of La^{3+} on HC oxidation over the 500°C sample appeared to be confined to the oxidation of propane in the propylene/propane feed. Propane oxidation over noble metal catalysts has previously been shown to depend on particle size (*18*), with large particles showing greater intrinsic rates than small particles. Thus our activity data suggest that Rh on the La^{3+}-containing catalyst is more highly dispersed than the catalyst without La^{3+}. This agrees with the CO chemisorption data for the 500°C oxidized catalysts, which yielded an apparent dispersion twice as high on the La-containing catalyst. The chemisorption results are supported by the XPS data. A simple analysis of relative XPS peak intensities (given in the Appendix) predicts mean Rh particle sizes that are consistent with the chemisorption data. The promoting effect of La^{3+} on Rh dispersion, qualitatively similar to that of Ce^{4+}, has been observed before (*10*) and also reported for Pt/γ-Al_2O_3 (*19*).

At oxidation temperatures above 500°C, La^{3+} exhibits additional effects beyond a simple promotion of Rh dispersion. As shown clearly by TPR, it blocks, to some extent, interaction of the Rh with the alumina support. Instead, the emergence of new TPR features suggests that a compound is formed between La and Rh. Collectively, the TPR and XPS data show that this compound is reduced in a temperature range intermediate between Rh_2O_3 and that Rh which is strongly interacted with alumina. Similar trends have been observed in studies of lanthanum rhodate compounds (*9, 11, 20*), which show that lanthanum rhodate reduces at temperatures between 200 and 600°C. The XPS data do not show direct evidence for the formation of a La–Rh compound, but the expected shifts are small enough and the peak broadening large enough that a chemical shift would be hard to discern.

The activity data obtained on the 800 and 900°C oxidized samples also suggest that La^{3+} forms a compound with Rh. Whereas La^{3+} primarily inhibited HC (i.e., propane) oxidation after 500°C oxidation, it strongly suppressed NO conversion and lean-side CO conversion after 800 and 900°C oxidation. Since CO oxidation and NO reduction are both less structure sensitive than propane oxidation, their inhibition by La^{3+}, relative to the Rh/γ-Al_2O_3 sample without La, appears consistent with the formation of a compound between Rh and La, which is catalytically less active than either the residual Rh left on the surface of the Rh/γ-Al_2O_3 catalyst or the Rh, which interacts with the alumina. Again, our data are consistent with a previous study of bulk Rh compounds (*9*), where, for example, lanthanum rhodate was shown to be less active than rhodium oxide.

Finally, it is interesting to note that both the Rh/γ-Al_2O_3 and Rh/La_2O_3/γ-Al_2O_3 catalysts could be completely restored to their fresh state by an 800°C reduction even after the 900°C oxidation. This argues against any significant sintering of Rh or deep penetration of Rh into the alumina under the conditions of this study. In fact, the long-term effect of Rh loss through reaction with γ-Al_2O_3 may not have been fully simulated

here, and it may thus be premature to draw conclusions as to the long-term influence of La^{3+} on this mode of deactivation in automotive exhaust.

In summary, this study shows that La^{3+} increases the dispersion of $Rh/\gamma\text{-}Al_2O_3$ catalysts and inhibits to some extent the interaction between Rh and the alumina under high-temperature oxidizing conditions. The mechanism by which it inhibits the Rh–alumina interaction appears to involve formation of its own compound with Rh. Under the reaction conditions examined here, this species is less active for HC, CO, and NO conversion than the Rh catalyst without La^{3+}. All of the structural and/or chemical changes induced in both the $Rh/\gamma\text{-}Al_2O_3$ and $Rh/La_2O_3/\gamma\text{-}Al_2O_3$ samples by high-temperature oxidation were completely reversed (at the level of resolution afforded by XPS, TPR, and catalytic activity measurements) by an 800°C H_2 reduction and reoxidation at 500°C. The results are in general accord with previous studies of high-temperature oxidation of $Rh/\gamma\text{-}Al_2O_3$ catalysts (*4, 5*), all of which have shown various levels of restoration depending on the severity of oxidation and reduction treatments.

APPENDIX

Consider the volume V of a sample probed by XPS and assume that it is characteristic of the whole sample. Let N be the number of Rh particles of average radius R contained in V, and denote the sample without (with) La^{3+} by subscript 1 (*2*). The total amount of Rh in V, proportional to NR^3, is approximately the same in both cases, so that

$$N_1R_1^3 = N_2R_2^3. \quad (1)$$

The total surface area of the Rh in V, proportional to NR^2, is different, however, by a factor of 2 according to the CO chemisorption results, so that

$$2N_1R_1^2 = N_2R_2^2. \quad (2)$$

The XPS intensity, proportional to NR^2L, where L is the smaller of $\{R, \lambda$ = electron inelastic mean free path ≈ 16 Å$\}$ in the limit of small ($R < \lambda$) and large ($R > \lambda$) particle, is different by the factor of 1.5, on the other hand, so that

$$1.5N_1R_1^2L_1 = N_2R_2^2L_2. \quad (3)$$

A nontrivial solution of Eqs. (1)–(3) obviously requires that neither limit (i.e., large or small particle) apply in both cases. Assuming, for the sake or argument, that opposite limits apply, with $R_1 > \lambda$ and $R_2 < \lambda$, Eq. (3) becomes

$$1.5N_1R_1^2\lambda = N_2R_2^3. \quad (4)$$

From Eqs. (2) and (4),

$$R_2 = (1.5/2)\lambda \approx 12 \text{ Å}, \quad (5)$$

and from Eqs. (1), (2), and (5),

$$R_1 = 2R_2 \approx 24 \text{ Å}, \quad (6)$$

marginally consistent with the initial assumptions. These particle radii, 12 and 24 Å, correspond to dispersions of about 30 and 15%, respectively, comparable to those deduced from the CO chemisorption measurements.

ACKNOWLEDGMENTS

The authors acknowledge K. Otto for help with the CO chemisorption measurements and analysis. The authors also thank M. Shelef, K. Otto, and J. deVries for useful discussions and a review of the manuscript.

REFERENCES

1. Pande, N. K., and Bell, A. T., *J. Catal.* **98,** 7 (1986).
2. Taylor, K. C., "Automobile Catalytic Converters." Springer-Verlag, New York, 1984.
3. Yao, H. C., Japar, S., and Shelef, M., *J. Catal.* **50,** 407 (1977).
4. Wong, C., and McCabe, R. W., *J. Catal.* **119,** 47 (1989).
5. Chen, J. G., Colaianni, M. L., Chen, P. J., Yates, J. T., Jr., and Fisher, G. B., *J. Phys. Chem.* **94,** 5059 (1990).
6. Fiedorow, R. M. J., Chahar, B. S., and Wanke, S. E., *J. Catal.* **51,** 193 (1978).
7. Yao, H. C., Stepien, H. K., and Gandhi, H. S., *J. Catal.* **61,** 547 (1980).
8. Rives-Arnau, V., and Munuera, G., *Appl. Surf. Sci.* **6,** 122 (1980).
9. Wan, C. Z., and Dettling, J. C., *in* "Catalysis and

Automotive Pollution Control: Proceedings of the First International Symposium'' (A. Crucq and A. Frennet, Eds.), p. 369. Elsevier, Amsterdam/New York, 1987.
10. Alvero, R., Bernal, A., Carrisona, I., and Odriozola, J. A., *Inorg. Chim. Acta* **140,** 45 (1987).
11. Tascon, J. M. D., Olivan, A. M. O., Tejuca, L. G., and Bell, A. T., *J. Phys. Chem.* **90,** 791 (1986).
12. Marvin, J. F. L., *J. Catal.* **123,** 245 (1990).
13. Bettman, M., Chase, R. E., Otto, K., and Weber, W. H., *J. Catal.* **117,** 447 (1989).
14. Shyu, J. Z., and Otto, K., *J. Catal.* **115,** 16 (1989).
15. Otto, K., *Langmuir* **5,** 1364 (1989).
16. Beck, D. D., and Carr, C. J., submitted for publication.
17. Oh, S. H., *J. Catal.* **124,** 477 (1990).
18. Otto, K., Andino, J. M., and Parks, C. L., submitted for publication.
19. Drozdov, V. A., Tsyrul'nikov, P. G., Popovskii, V. V., Pankrat'ev, Yu. D., Davydov, A. A., and Moroz, E. M., *Kinet. Catal.* **27,** 721 (1986). [In Russian]
20. Gysling, H. J., Monnier, J. R., and Apai, G., *J. Catal.* **103,** 407 (1987).